Adaptive sampling for sand bank mapping using an autonomous underwater vehicle equipped of an altimeter

Maria João Rendas[(1)], Isabel M. G. Lourtie[(2)], Georges Pichot[(3)]

[(1)] Laboratoire d'Informatique, Signaux et Systèmes de Sophia Antipolis, 2000 rte des Lucioles, BP. 121, 06903 Sophia Antipolis cedex, France. E-mail:rendas@i3s.unice.fr

[(2)] Instituto de Sistemas e Robótica, Instituto Superior Técnico, Torre Norte, Av.Rovisco Pais 1049 - 001 Lisboa, Portugal. E-mail: iml@isr.ist.utl.pt.

[(3)] MUMM, Management Unit of the North Sea Mathematical Models, Gulledelle 100, 1200 Brussels, Belgium. E-mail: pichot@mumm.ac.be.

ABSTRACT

This paper describes adaptive sampling of the bathymetry of a prescribed area using an inexpensive autonomous vehicle equipped of a bathymetric sensor. The proposed mapping approach should not be understood as an alternative to the present use of oceanographic vessels equipped of sophisticated sensors, but rather as a complementary observation tool, enabling rapid, inexpensive and frequent observation of areas under study. In some sense, the high quality of traditional surveying techniques is traded for the possibility of achieving a denser temporal sampling, and direct acquisition of relevant surface features, which may be important to enable analysis of impact of temporally localized perturbations, like storms, or of external (human) intervention in a given area. The work described has been carried out in the context of the EU funded (IST program) project SUMARE – acronym for Survey of Marine Resources – that develops adaptive sampling techniques for the observation and monitoring of marine resources. More precisely, the project considers two different applications: mapping of maerl habitats in Orkney, Scotland, and mapping of the bathymetry of the Kwintebank, off the Belgium coast. This bank has been subjected to intensive extraction of sand. To ensure the sustainability of this resource, surveying campaigns are regularly conducted using an oceanographic vessel, producing bathymetric profiles at a set of fixed tracks, historically based on navigation DECCA lines. The cost of the surveying means used to acquire these profiles restricts achievable sampling over both the temporal and spatial domains, making it difficult to establish the correlation of observed sand volume variations along distinct tracks, and to identify the exogenous factors that explain the observed variations. In the paper we describe an autonomous underwater vehicle equipped of a bathymetric sensor and with limited autonomy, which is able to directly acquire maps of level lines (lines of constant depth) of the sea-floor, and to follow gradient lines (lines of steepest slope). Extension of the present system to acquire a complete bathymetry map of a bounded region is discussed. In the paper we describe the architecture of the system, and present examples of simulated missions using real bathymetry maps of the Kwintebank (multi-beam maps provided by MUMM).

I. Introduction

This paper discusses autonomous acquisition of bathymetric maps using unmanned underwater platforms. Bathymetry maps are important tools for both physical oceanography studies – e.g the effect of tides and currents on the morphology of coastal areas – as well as for practical applications, such as extraction of sand and gravel for civil engineering. The work reported here is motivated by the need of controlling the amount of sand extracted from underwater dunes in the Belgian marine zone of the North Sea, to guarantee the sustainability of the resource, in particular to prevent dune collapse, which could lead to modifications of the present equilibrium, with strong impact at both social and economic levels

on the life of coastal communities. The Belgium institute MUMM (Management Unit of the North Sea Mathematical models) is responsible for assessing the impact of on-going exploitations on the total amount of sand. To this end, surveys are conducted using the oceanographic vessel *Belgica*, presently equipped of a multi-beam sonar, being in this way able to produce detailed and complete maps of the underwater relief. This application as been selected by the SUMARE[1] project as one of the two test-beds on which the project's results on the development of adaptive sampling techniques for environmental observation using autonomous underwater vehicles should be tested.

When assessing the acquisition of environmental information with autonomous platforms, instead of oceanographic survey vessels, one can exploit the ability of the platform to react on-line to observed data. The platform's trajectory, and thus the sensor path, can in this way be determined adaptively, instead of being pre-specified, as it is the case for traditional survey means. In the case of the SUMARE application, bathymetric data is presently acquired by mapping the profiles of the sand dunes along a series of parallel transects. The evolution of the dunes is then assessed by analyzing the dunes' elevation along these profiles, in order to detect regions where there is significant variation (more precisely, it is important to detect regions where the volume of sand is decreasing). This sampling design does not seem to be able to provide sufficient information to check in due time that sustainability criteria are fulfilled or to assess the interesting problem of *evolution* of the *global shape* of the dunes.

In the SUMARE project we are interested in studying the possibility of directly acquiring maps of specific topological features of the sea floor surface. While this seems difficult using traditional surveying methods, it corresponds to natural perception-driven modes for autonomous robots. In this paper, we present perception-driven guidance laws for adaptive observation, as an alternative to regular surveying patterns.

The paper is organized as follows. The next section motivates our mapping strategy, and identifies the guidance modes that it requires. Section III presents the control architecture of the vehicle and defines the relevant observation equations. Sections IV and V, are dedicated to the formal presentation of our solution to two guidance problems: tracking of iso-depth lines and gradient following. Section VI presents simulation studies using a real bathymetric map of the Kwintebank, validating the proposed algorithms. Finally, section VII summarizes the major results presented, and lists directions for future research.

II. Mapping strategy

We consider the problem of *acquiring bathymetry maps of extended areas of the ocean floor*. In particular, the areas of interest in this study are very shallow (depth can be as small as 5 meters) and have a hilly detailed topography, as shown in Figure 1. The very shallow conditions impose strong limitations to the operation of oceanographic vessels, which require a minimum sea depth for safe operation, and are one of the factors that make the alternative use of autonomous vehicles attractive.

It is evident that the complete observation of extended ocean regions is extremely time consuming and cannot be done routinely, imposing some form of *spatial sub-sampling* of the actual 3D surface that is defined by the ocean depth at each point. A sampling strategy must then be identified, defining the points that will actually be mapped. Traditionally, as we said before, the necessary degree of sub-sampling is achieved by specifying a regular pattern that imposes a certain spatial frequency of observation. Since the path of a vessel is necessarily a continuous 1 dimensional curve, which for oceanographic vessels is contained in the sea surface, the observation pattern is normally defined by choosing a certain "scanning" direction, based on prior knowledge of the fields' characteristics, and a sampling frequency along the orthogonal direction. This imposes an *homogeneous* minimal spatial frequency of the field's sampling. This traditional survey design has been systematically used even with autonomous underwater platforms, see for instance [3]. The homogeneous nature of this sampling design does not seem appropriate for natural fields, which are, most often, strongly inhomogeneous. A more efficient use of the sensor should concentrate the measures in regions of high variability, while making sparser observations in flat areas.

[1]SUrvey of MArine REsources, see http://www.mumm.ac.be/SUMARE for more information.

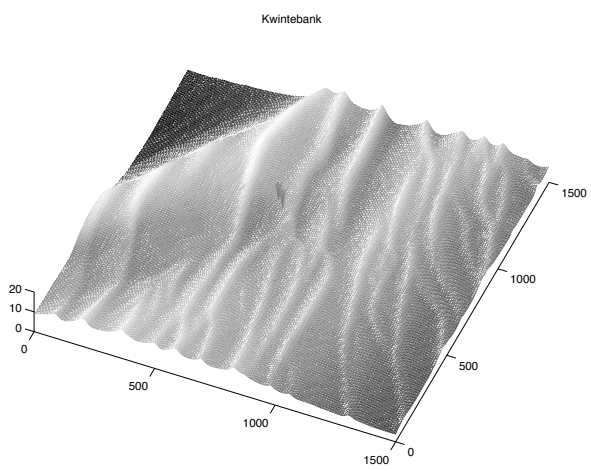

Fig. 1. Bathymetry of the Kwintebank

Fig. 2. Mauve.

This variable sampling requires an adaptive behavior of the sensor, which must define its trajectory on-line, in terms of the observed local characteristics of the monitored field. While this seems difficult in the context of the operation of large oceanographic vessels, it is a possible mode of operation for small autonomous vehicles, like the vehicle MAUVE[2], shown in Figure 2. As an alternative to the fixed survey designs mentioned above, an appropriate spatial sampling is obtained if we require the vehicle to *track lines of constant sea depth*: it is well known that contour lines of a surface are denser in the regions of strong variability of the surface, and are sparse in flat regions.

Observation of a single contour line is not enough to define the geometry of the sea floor surface over a given bounded area M. We briefly address below the problem of defining a complete mapping approach, which will be fully assessed in a future publication. Our approach is based on the assumption that the ocean's surface is, inside the bounded support M, a Morse function, i.e., that all its critical points are non-degenerate [1]. The critical points of a function $f : M \subset \mathbb{R}^2 \to \mathbb{R}$ are the points at which its gradient vanishes. A critical point is degenerate if the Hessian (the matrix of second derivatives) is singular at that point. Non-degenerate critical points can be classified in three types, according to the sign of the eigenvalues of the Hessian matrix at that point: *(i)* it is a maximum if both eigenvalues are negative, *(ii)* a minimum if both are positive, and a saddle point otherwise. Saddle points are special in that there are four particular slope lines that emanate from them: two emanate in the steepest ascent direction and are called *ridges* and the other two emanate in the steepest descent direction and are called *rivers*. Each cycle of rivers delineates an area called a *hill*, which has a single local maximum. The region M can thus be tesselated into either dales or *hills*, such that each point belongs exactly to one dale and one hill. Dales have a unique minimum and hills a single maximum. It is known from Morse theory [1] that the topography of a Morse function can be completely captured by the *critical point configuration graph* (CPCG) []. The nodes of this graph are the critical points, and the edges are ridges and rivers, such that

- a maximum can be connected (by a ridge) to a minimum or to a saddle point
- a saddle point is connected (by a river) to either another saddle point or to a minimum.

The critical point configuration graph allows us thus to partition a region into disjoint areas, inside which the topology of the surface is simple.

The contour lines (also called level lines) are lines of constant value of f. Through each regular point there is a single slope line and a single level line, and they are orthogonal at the point considered. The

[2]Miniaturized Autonomous Underwater Vehicle for costal Exploration.

shape of a contour line is locally perturbed in the intersection with rivers and ridges. More specifically, the curvature of a contour line is concave upwards a river and convex for ridges.

Determination of the critical point configuration graph representing a given region M, together with their relative heights, determines the complete set of contour lines that are required to map the surface with a given resolution. Note however, that determination of this graph is critically dependent on the ability to map the *saddle points*, since the ridges and rivers emanate from them. Unfortunately, the saddle points, contrary to maxima and minima, are not attraction points of the guidance laws proposed in this publication, meaning that our controllers are not able to use the surface topology to drive the vehicle towards them. However, if some contour lines have already been mapped, we can exploit the remark on the previous paragraph to search for possible saddle points.

An alternative representation to the critical point configuration graphs as been proposed recently in the field of computational geometry [**?**]: the *Contour Tree*. In this tree, the nodes correspond to the critical points (either maxima, minima or saddle points) and the arcs are classes of equivalence of contour lines. The maxima and minima are the leaf nodes of the tree, while the saddle points are always inner nodes, and they can be split into *joins*: saddle points at which two distinct equivalence classes of contour levels join to form another equivalence class or *splits*, where the oppposite happens: one equivalence class splits into two disjoint equivalence classes. In this representation, and equivalence class of contour levels gathers nested contour lines, necessarily belonging to the basin of attraction of the same maximum or minimum. Our adaptive sampling strategy uses the local geometry of the observed field to iteratively built the contour tree that describes it. Lack of space prevents its full presentation here. Informally, we can say that the approach is based on completely exploring the interior of each contour level already mapped before attempting to map its exterior region, and on the principle of proceeding from the leaf nodes towards the interior of the contour tree. Decision of whether a given "basin" has been completely mapped, and exploitation of its interior is based on criteria about the geometry of mapped contour lines. A simplified description of autonomous mapping algorithm is given below.

1) **initialize:** start with an empty contour tree graph, and an empty list of basins under mapping.
2) **exploit: find a critical point** by tracking a slope line form the current position $C_{d_0} = \{f(x, y) = d_0\}$.
3) **characterize** classify the previous singular point (maximum, minimum or saddle point). If the singular point is
   - a new saddle point, create the corresponding *split* or *join* in the contour tree;
   - a new extremum (either maximum or minimum), insert a new leaf node in the contour tree, and go to the next state.
   - if it is already in the map, select a new position to do another exploitation of the basin. If no such position can be found, delete this basin from the list and resume the exploration of the most recent element of the list of unfinished basins. If this list is empty, exploit the exterior of a mapped basin.

   If it is maximum or minimum, go to next state
4) **basin mapping:** By incrementally updating the reference depth, acquire the level lines belonging to the basin of attraction of the most recently found leaf node. For each new level line, test for the possible presence of unmapped extrema or saddle points inside this basin. If the text is positive, select a starting point to search for the singular point, and move to the first step, inserting the current basin in a list of basins under mapping.

The brief discussion below shows that adaptive strategies for mapping the bathymetry of a region are naturally defined in terms of two basic tasks: **tracking of iso-depth lines** and **tracking of lines of steepest slope** (either ascending or descending). In the present version of MAUVE, the mapping strategy outlined above is not yet implemented. Instead, the user can specify the depth(s) of the level line(s) that must be mapped. From its launching point, the AUV autonomously searches for the specified depth along paths of steepest slope. Upon detection of the target depth, the level line is mapped. A maximum distance is

Fig. 3. Problem geometry

predefined, which if attained before detection of the target level line, triggers mission abortion, and return of the vehicle to the launching point.

III. General Architecture

This section presents the equations that model the measurements available at the vehicle, giving their dependence on position and attitude of the vehicle relative to the sea bed surface. The simplifying assumptions under which we develop the two guidance algorithms of subsequent sections are presented. The control architecture is detailed, presenting its dependence on the low-level control loops of the vehicle (the *auto-pilots*) and addressing also the high-level (event driven) execution control problem.

A. Sensor measurements

Let $h(x, y)$ denote the bathymetry (sea depth) surface at position x, y (in a Cartesian global frame), and let x_k, y_k, z_k denote the position, and θ_k, ψ_k, and ϕ_k attitude angles (yaw, pitch and roll) of the robot at time instant t_k. The altimeter measurements represent, in the body frame, the distance d_k of the vehicle to the sea bottom. At position x_k, y_k, z_k the vehicle samples a point in the ocean bottom with coordinates x_{in_k}, y_{in_k}, $h(x_{in_k}, y_{in_k})$ – see figure 3 that illustrates the problem geometry in the vertical plane aligned with the direction of motion, assuming a zero roll angle – given by

$$\begin{bmatrix} x_{in_k} \\ y_{in_k} \\ h(x_{in_k}, y_{in_k}) \end{bmatrix} = R_{yaw}^T R_{pitch}^T R_{roll}^T \begin{bmatrix} 0 \\ 0 \\ d \end{bmatrix} + \begin{bmatrix} x_k \\ y_k \\ z_k \end{bmatrix}, \tag{1}$$

where R_{yaw}, R_{pitch} and R_{roll} are the rotation matrices along the axis of the body frame.

We assume that the three attitude angles are measured with small errors, for instance by a three axis compass, or one compass and an inclinometer, as it is the case for the vehicle Mauve. As we will see in the next sections, our guidance algorithms do not require estimation of the horizontal coordinates of the sample point, x_{in_k} and y_{in_k}, and depend only on the evolution of the total measured altitude $h(x_{in_k}, y_{in_k})$. We assume that the vehicle is naturally stabilized in roll, such that $\phi_k \equiv 0, \forall k$. In this situation, the altitude measures are approximately given by

$$h(x_{in_k}, y_{in_k}) \simeq \cos(\varphi_k) d_k + z_k. \tag{2}$$

This shows that we should map the terrain with a trajectory as close as possible to the sea bottom, to minimize the impact of pitch oscillations, taking into account the smoothing effect induced by the non-zero beamwidth of the altimeter. The altitude measures fed to the guidance algorithms presented below should thus be understood as the corrected measures given by eq. (2), using the measures of the pitch sensor.

We assume that during map acquisition the depth of vehicle is controlled either at constant depth (during tracking of contour lines) or at constant altitude (during transition between iso-depth lines). In this way, pitch variations, which directly map into noise in the altitude measures, are minimized. From the point of view of the guidance problems studied below this is irrelevant, since the relevant measure is the sum of both depth and altitude corrected by the measured pitch value.

B. Control architecture

The body motion of the vehicle is controlled using three decoupled control loops: closed-loop depth/pitch controllers and heading/rate controllers and open-loop surge controller. Both pitch and rate controllers can be directly used, or their reference signals generated by outer control loops which receive reference values for depth and heading, respectively. An external signal (*mode*) selects which input will be used as reference for the inner (pitch and rate) controllers. This external signal can assume the following logical values

- *trajectory reference*: in this case the pitch reference is taken from the depth controller, and the rate reference from the heading controller;
- *line tracking*: the pitch reference is generated by the depth controller from the desired constant value of the vehicle's depth, the rate reference is the output of the K_{line} controller described in the next section;
- *gradient following*: the pitch reference is generated by the depth controller, from a desired value of the vehicle's altitude, while the rate reference is generated by the K_{grad} guidance algorithm presented in section V.

We assume that in all modes, the surge velocity of the vehicle is held constant. When the basic control loops are active, and after detecting the h_{ref} level line to be tracked, the closed-loop contour tracker is responsible for generating the rate reference signal to be imposed to the rate control system.

IV. Control Algorithms

We present in this section the guidance algorithm for tracking lines of a reference depth of the sea floor.

As presented in the previous section, the guidance algorithms for the two perception-driven behaviors considered in this paper directly act on the vehicle's angular rate. For constant surge velocity, u_k, this is equivalent to controlling the trajectory curvature $\mathcal{K}$ at each point:

$$\mathcal{K} \triangleq \frac{d\theta}{d\ell} = \frac{d\theta}{dt}\frac{dt}{d\ell} = \frac{r_t}{u_t} \ . \tag{3}$$

According to the differential approach to the definition of a general one-dimensional curve in $\mathbb{R}^2$, specification of the curvature at each point uniquely identifies a given planar curve. Recognizing this fact, we will search the controllers' structures by imposing a family of trajectories as local solutions to eq. (3), under simplified assumptions with respect to the local geometry of the sea bed (local planarity, which is approximately verified for all smooth 2-dimensional manifolds except at singular points). Obviously, different families will be chosen for the two behaviors under study. In this section we define the iso-depth line tracker. The tracker of lines of maximal slope (gradient tracker) is studied in the subsequent section.

To define the contour tracking mission using altitude measures, the following parameters need to be specified (input parameters):

1) u_{ref} – vehicle's surge velocity;
2) z_{ref} – vehicle's depth;
3) h_{ref} – altitude of the iso-depth bathymetric line to be tracked;
4) $\mathcal{S}$ – indicates if the vehicle must turn left ($\mathcal{S} = -1$) or right ($\mathcal{S} = +1$) once the iso-depth line to be tracked is detected.

The first two parameters select one of all possible solutions to eq. (3), defining the value of the constant $u_t = u_{ref}$ in this equation, and selecting the 3-dimensional plane in which the trajectory is contained: $z = z_{ref}$. The two last parameters characterize the contour tracking task.

Consider a non-singular point of the sea-bed surface $p = (x, y, h_ref)$ on the tracked line, and the associated tangent plane, T_p. Since p is a regular point, T_p has a non-zero slope. We impose that the vehicle trajectory in the horizontal plane containing the tracked level line approximates a *damped sinusoid*. Consider the coordinate system around point p defined by the normal (n_p) and velocity (v_p) vectors of the

curve at point p, Span$\{v_p, n_p\}$. Denote the unit vectors along these two directions by $x = v_p$ and $y = n_p$. The imposed trajectory is then of the form

$$y(x) = A\sin(fx)e^{-\alpha x} \ , \tag{4}$$

for some constants A, f and α.

The admissible solutions must satisfy the kinematic equations of the (center of gravity) vehicle at each point. For constant surge velocity, and assuming that the vehicle's sway is identically zero, the following equations must thus hold at each point of the trajectory:

$$\frac{dx_\ell}{d\ell} = \cos\theta_\ell, \qquad \frac{dy_\ell}{d\ell} = \sin\theta_\ell, \qquad \frac{d\theta_\ell}{d\ell} = r_\ell \ , \tag{5}$$

since, for constant u, we have $d\ell = u\ dt$. To determine the controller's structure, we search the value of r_ℓ that leads to trajectories of the form (4). Derivating $\frac{dy(x)}{dx} = \tan\theta$ w.r.t. ℓ, and taking into account (5), we obtain after some algebraic manipulations

$$r_\ell = \frac{d\theta_\ell}{d\ell} = -\left(\alpha^2 + f^2\right)\cos^3\theta_\ell y_\ell - 2\alpha\cos^2\theta_\ell \frac{dy_\ell}{d\ell} \ . \tag{6}$$

This equation gives us r_ℓ as a function of the vehicle's coordinate in the direction of the normal, y_k.

The discrete time (Euler) equivalent of the equation above is

$$r_k = -u\left(\alpha^2 + f^2\right)\cos^3\theta_k y_k - 2\alpha\cos^2\theta_k \frac{y_k - y_{k-1}}{\Delta T} \ . \tag{7}$$

Using the approximation of the sea floor by the tangent plane,

$$h(x, y) = \rho y + h_{ref} \tag{8}$$

where ρ is the terrain slope, and we can write (7) directly in terms of the sea depth h_k at the current point:

$$r_k = K_P\left(h_{ref} - h_k\right) - K_D\left(h_k - h_{k-1}\right) \ , \tag{9}$$

where we defined

$$K_P = \frac{u\left(\alpha^2 + f^2\right)}{\rho}\cos^3\theta_k, \qquad K_D = \frac{2\alpha}{\rho\Delta T}\cos^2\theta_k \ . \tag{10}$$

We conclude that the curvature should vary proportionally to the altitude error $h_{ref} - h_k$ and to its first order differences $h_k - h_{k-1}$. If K_P and K_D were constants, eq. (9) would be a standard discrete proportional-derivative controller. As eq. (10) shows, the gains K_D and K_P are time-varying, depending on θ_k, the angle between the vehicle's velocity and the line being tracked. A time-invariant linear solution can be obtained by considering that θ_k is small $\forall k$, i.e., by making

$$K_P^{ap} = \frac{u\left(\alpha^2 + f^2\right)}{\rho} \qquad \text{and} \qquad K_D^{ap} = \frac{2\alpha}{\rho\Delta T} \ . \tag{11}$$

Denote by r_k^{ap} the solution of eq. (9) using these constant gains, and by $(x_{,k}\, y_k)^{ap}$ the resulting trajectory. For $-\frac{\pi}{2} < \theta_k < \frac{\pi}{2}$, r_k^{ap} is larger than r_k leading to a trajectory that always lies closer to the contour than the solution of equation (7), i.e., $|y_k^{ap}| \leq |y_k|$. The simpler linear controller yields thus a trajectory that is closer to the iso-depth line than the initially imposed curve (4). For this reason, we adopt (9) for the structure of the guidance algorithm, with the constant gains given by (11). Equation (11) solves the synthesis problem, showing that to achieve a given damping ratio α and spatial frequency of oscillation along the contour, f, the controller gains depend also on the mission velocity u, terrain slope ρ and control rate ΔT. The parameters α and f are not the natural design parameters for a contour tracking task. The damped sinusoidal trajectory can alternatively be characterized by the parameters L_1, L_2, L_3 represented in Figure 4. Taking into account the expression of $y(x)$, it is easy to show that

$$L_2 = \frac{\pi}{f} \qquad \text{and} \qquad \frac{L_3}{L_1} = e^{-\alpha\frac{\pi}{f}} \tag{12}$$

Fig. 4. Approximate (linear model) trajectory in green, and trajectory given by the damped sinusoid

i.e.,

$$f = \frac{\pi}{L_2} \qquad \text{and} \qquad \alpha = \frac{1}{L_2} \ln\left(\frac{L_1}{L_3}\right) \tag{13}$$

The above relationships allow us to specify the frequency of oscillation of the trajectory around the contour (L_2 represents half of a period of the damped sinusoid) and the damping rate (which is characterized by the ratio L_3/L_1). However, the maximum deviation between the trajectory and the contour (L_1) cannot be fixed since it depends on the amplitude A of the damped sinusoid which is determined by the angle of arrival, θ_0:

$$A = \frac{1}{f}\tan\theta_0, \qquad L_1 = \frac{\tan\theta_0}{f\sqrt{(\alpha/f)^2+1}} e^{-\frac{\alpha}{f}\arctan\left(\frac{f}{\alpha}\right)} . \tag{14}$$

Remark that θ_0 is the angle between the trajectory and the contour at the first crossing point, which is not known a priori. This means that we can impose a given spatial period L_2 and a given damping L_3/L_1, but it seems that we cannot control the maximum excursion L_1. It actually can be shown that L_1 has a linear dependency on θ_0, and that a worst-case analysis can be used to overcome lack of knowledge of θ_0, enabling convenient design of all gains,

$$L_1 < \frac{\pi}{2\sqrt{\alpha^2+f^2}} e^{-\frac{\alpha}{f}\arctan\left(\frac{f}{\alpha}\right)} . \tag{15}$$

Simulation studies of this algorithm for realistic bathymetry surfaces are presented in section VI, demonstrating that it can effectively handle non-planar surfaces. Before, we address in the next section the definition of a guidance algorithm to track lines of maximum slope of the sea-bed surface, enabling proper transition between iso-depth lines when mapping a given area.

V. Moving along the gradient

We address now the problem of guiding the vehicle along the gradient of the sea-bed surface, i.e., along lines of maximum slope. We assume that the following parameters are specified:

1) u_{ref} – vehicle's linear velocity;
2) d_{ref} – vehicle's altitude.

To design the control law that drives the vehicle along lines of maximum increasing altitude gradient, we consider again the approximation of the surface at a given point by its tangent plane T_p, eq. (8), with iso-depth lines parallel to y. In this case, our goal is to keep the vehicle aligned with the gradient vector. The surface slope is not directly measured, and we can observe it only through the slope along the direction of motion

$$s_\ell = \frac{dh}{d\ell} = \rho\frac{dy}{d\ell} \tag{16}$$

In the particular geometry considered, the control objective is met by any trajectory parallel to the y coordinate.

We impose that (under the local planar geometry assumed) the guidance algorithm leads to a vehicle trajectory with a exponential convergence towards the desired direction:

$$x(y) = B\left(1 - e^{-\beta y}\right). \tag{17}$$

Note that along this curve, $\theta_k > 0, \forall k$, and thus that this model cannot describe the vehicle's behavior when the vehicle is initially aligned along a line of decreasing depth. This case will be studied separately.

Fig. 5. Tracking a line of large curvature (noise).

Fig. 6. Tracking a line of large curvature (no noise).

Assuming as before that u is constant, computing the first derivative of $dx/dy = \tan^{-1}\theta$ w.r.t. arc length ℓ, noting that

$$\frac{ds_\ell}{d\ell} = \rho \cos\theta_\ell r_\ell \ , \tag{18}$$

and taking into account the kinematic equations (5), we obtain

$$r_\ell^2 = \beta \sin^3\theta_\ell \frac{d\ln(s_\ell)}{d\ell}. \tag{19}$$

The discrete time equivalent of the above equation, for constant u, such that $r_t = ur_\ell$, and assuming that θ_t is smaller than $\pi/2\ \forall t$, is

$$r_k^2 = \frac{u\beta \sin^3(\theta_k)}{\Delta T}\left(\ln\frac{s_k}{s_{k-1}}\right) \leq \frac{u\beta}{\Delta T}\left(\ln\frac{s_k}{s_{k-1}}\right) \ . \tag{20}$$

If we drop the dependency on $\sin^3\theta_k$, we obtain thus a difference equation whose solutions necessarily lie closer to the line $x = x_0$ than (17).

Control law (20) will drive the vehicle along the trajectories for which the slope derivative along motion, $ds_\ell/d\ell$, vanishes. For the simplest case of a planar environment, the slope variation along any straight line is zero, meaning that variations on the terrain slope are not observable when the vehicle is moving on a linear trajectory. To overcome this problem, and improve observability of the altitude gradient, we consider an additional term in the control law to perturb the vehicle's motion around the exponential nominal trajectory (17). The resulting control law becomes

$$r_k = \sqrt{\left|\frac{u\beta}{\Delta T}\ln\left(\frac{s_k}{s_{k-1}}\right)\right|}\mathcal{D} + p_k \ , \tag{21}$$

where p_k is the perturbation signal

$$p_k = S_L \mathrm{rect}_{N_p}\left(k + \frac{N_p}{4}\right), \tag{22}$$

and $\mathrm{rect}_{N_p}(k)$ stands for the rectangular waveform with period $4N_p$. Parameter $\mathcal{D}$ should be taken as $\mathcal{D} = \mathrm{sign}(r_{k-1})$ if the vehicle is moving toward increasing altitude gradient and $\mathcal{D} = -\mathrm{sign}(r_{k-1})$ when the slope along the vehicle's heading is negative.

VI. Simulations

We present in this section simulation studies that illustrate the behavior of the proposed guidance algorithms for realistic bathymetry maps. All case studies presented consider the complete simulation of the dynamic model of the underwater vehicle (including thrusters), together with its existing low-level control loops. Only the motion in the horizontal plane is simulated, an vehicle speed is 1 ms^{-1}.

Figure 5 shows the ability of tracking lines of large curvature. For this simulation a small level of noise has been added to the altimeter measurements (Gauss distribution with standard deviation equal to 1 cm). As it should be expected, the gradient tracking algorithm is the one most perturbed by the presence of noise, as we can conclude by comparing this Figure with the trajectory obtained for noiseless measures, shown in Figure 6. Figures 7 and 8 show simulation of the mapping of a larger level line, again under distinct noise conditions. Since the estimated slope which is used to compute the values of the gains K_P

Fig. 7. Tracking a longer level line (no noise).

Fig. 8. Tracking a longer level line (strong noise).

and K_D depends on the approaching angle (being smaller for the noisy case), the vehicle's trajectory during tracking is different, displaying a more oscillating behavior for the noisy cases. Solving for this problems requires adaptive adjustment of the controller gains, based on adaptive estimation of the surface slope during contour line tracking, and is the subject of current studies.

VII. Conclusions

The paper presented work on the definition of adaptive sampling strategies to acquire bathymetry maps using an autonomous underwater vehicle, based on two complementary observation modes: tracking of iso-depth lines, and tracking of slope lines. The control algorithms presented are currently under implementation in the AUV Mauve.

The controllers proposed automatically adjust to the topographic conditions of the observed region. Namely, the controller gains during tracking of iso-depth lines use the slope estimated during the approaching phase (when tracking lines of slope). The current implementation keeps these gains fixed during the entire observation of a given iso-depth line. This design can be improved, by considering estimation of the terrain slope adaptively, during tracking of a given level line. This issue will be studied in the near future.

The complete implementation of the observation strategy outlined in section II is not done in this paper, and will be the subject of a future publication, which will also address the issue of detecting the critical points of the surface, and classify them either as maxima/minima or as saddle points. Another open problem concerns the detection of the critical points (maxima, minima and saddle points), which is at the base of the definition of the CPCG. Robust detection of these points will be addressed in the near future. Finally, an issue of *scale* must be assessed: a real terrain exhibits a high number of local maxima, minima and saddle points, defining a fine partition of the support region M. A feasible mapping strategy should concentrate on mapping only features of a given user-defined scale. The precise definition of how this scale should be indicated by the user, and how it should be used during mapping has not yet been made. A possible approach is to consider the use of Laplacian or Gauss filters, together with delayed decision schemes.

Acknowledgements

This work has been partially funded by the European Union through IST project SUMARE (*Survey of Marine Resources*).

References

[1] Milnor, J.: Morse Theory, Princeton University Press, New Jersey, 1963

[2] Nackman, L.R., Two Dimensional Critical Point Configuration Graphs, IEEE Trans. on Pattern Analysis and Machine Intelligence, PAMI-6, No.4, pp:442-450, 1984.

[3] Yoerger, D., Bradley,A., Cormier, M.-H., Ryan, W., and Walden, B., High Resolution Mapping of a Fast Spreading Mid Ocean Ridge with the Autonomous Benthic Explorer, Proc. of the 11^{th} Symposium on Unmanned Submersible Technology, Durham, NH, August 1999.